Composition Dependent Magnetic Properties of Ni-Co-P Coated Carbon Nanotubes

2009 Chin. J. Chem. Phys. 22 411

(http://iopscience.iop.org/1674-0068/22/4/12)

ARTICLE

Composition Dependent Magnetic Properties of Ni-Co-P Coated Carbon Nanotubes

Min Ye[a,b*], Ting Xie[a,b], Bao-lin He[c], Yu-cheng Wu[a,c], Guo-wen Meng[a], Li-de Zhang[a]

a. Key Laboratory of Materials Physics, Institute of Solid State Physics, Chinese Academy of Sciences, Hefei 230031, China
b. Institute of Tribology, Hefei University of Technology, Hefei 230009, China
c. School of Materials Science and Engineering, Hefei University of Technology, Hefei 230009, China

(Dated: Received on March 2, 2009; Accepted on April 13, 2009)

Carbon nanotubes were coated with a layer of nickel-cobalt-phosphorus (Ni-Co-P) alloy with different compositions of Ni/Co through electroless plating. The effects of the concentration ratio of Co^{2+} to Ni^{2+}, bath temperature, and pH on deposition rate are discussed. The prepared carbon nanotubes covered with Ni-Co-P were characterized and analyzed by field-emission scanning electron microscopy, transmission electron microscopy, X-ray diffraction, energy dispersive spectroscopy, and a vibrating sample magnetometer. The results show that the deposition rate reached the maximum when the concentration ratio of Co^{2+} to Ni^{2+} is 1 and the pH is 9; the deposition rate increases with the increase of bath temperature. The measurements of the magnetic properties of the obtained carbon nanotubes covered with Ni-Co-P indicate that the magnetic properties greatly depend on the concentration ratio of Co^{2+} to Ni^{2+}, and the magnetic saturation reaches the maximum value when the Co^{2+} to Ni^{2+} ratio is 1. In addition, there are two peaks in the coercivity curve at Co^{2+} to Ni^{2+} ratios of 1/2 and 4/1, while the two peaks in the magnetic conductivity curve are located at Co^{2+} to Ni^{2+} ratios of 1/4 and 4/1.

Key words: Ni-Co-P, Carbon nanotube, Electroless plating, Composition, Magnetic property

I. INTRODUCTION

Since the first observation at the beginning of 1990s by Iijima [1], carbon nanotubes (CNTs) have been the focus of considerable research because of their outstanding structural, mechanical, and electronic properties [2]. They have applications in molecular electronics [3], chemical sensors [4], scanning probes [5], supercapacitors [6], energy storage devices [7], and so on. In order to give the CNTs more attractive functional features, in recent years, various approaches were developed to obtain CNT composite structures, such as doped the CNTs [8,9], filled the CNTs with metals [10,11] or compounds [12], and coated and modified CNTs [13–15] to meet the needs of various applications in nanodevices and nanocomposites [16,17]. In particular, the surface modification of CNTs with metals or alloys has been reported in many publications. Generally, the CNTs were coated with metals or alloys through the following routes: wet chemistry [18,19], *in situ* reduction [20], electron-beam deposition [21], and electroless plating [22,23].

Because Ni-Co alloy is an important magnetic material, there has been considerable interest to explore the synthesis of the Ni-Co alloy nanoparticles [24,25], nanofilms [26,27], and nanowires [28,29] due to their potential applications in the ultra-high-density magnetic storage devices, microsensors and automotive industries [30–32]. Ni-Co alloy coatings on CNTs are believed to combine the advantages of both Ni-Co alloy and CNTs, which are very important promising materials used in nanodevices. So far as we know, only a few related researches have been reported. Wu *et al.* obtained $Fe_xCo_yNi_{100-x-y}$ alloy nanoparticles with controllable compositions attached on the surface of CNTs using an easy two-step route including adsorption and reduction processes [19], Li and his co-workers prepared Ni-Co-P coated SiC powders by electroless plating [33]. In the present work, electroless deposition was employed to synthesize the Ni-Co-P coatings with alternating compositions on CNTs. It was focused on understanding the influence of Co/Ni content on the magnetic properties of the coatings. The effect of the deposition parameters on the formation of the coatings is discussed. The morphology and structure of Ni-Co-P coatings on CNTs were also investigated.

*Author to whom correspondence should be addressed. E-mail: minye_hfut@yahoo.cn

TABLE I Electroless plating solution and operating conditions of Ni-Co-P alloy coating on MWCNTs.

Electroless plating solution		Operating conditions
Component	Concentration/(g/L)	
$NiSO_4{\cdot}6H_2O$ (salt)	4–22	Bath temperature: 20–30 °C
$CoSO_4{\cdot}6H_2O$ (salt)	5–24	pH=8.5–8.8
$NaH_2PO_2{\cdot}H_2O$ (reducer)	30–38	Deposition time: 40–50 min
$Na_3C_6H_5O_7{\cdot}2H_2O$ (complex agent)	80	Agitation (ultrasonic and mechanical)
$(NH_4)_2SO_4$ (buffer agent)	50–60	Addition of surfactant

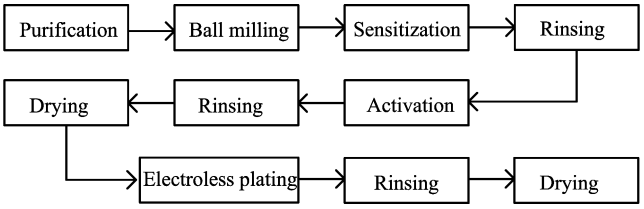

FIG. 1 Processes of the electroless deposition of Ni-Co-P alloy coating on MWCNTs.

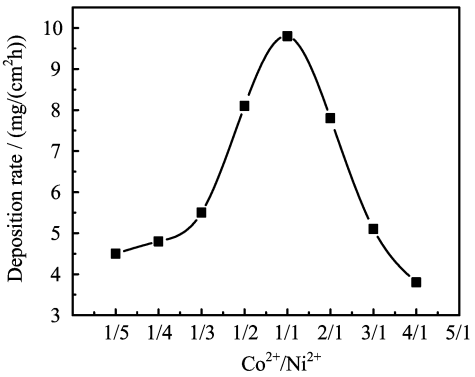

FIG. 2 Relationship between the deposition rate and Co^{2+}/Ni^{2+} value, when the solution pH value is 8.5, bath temperature is 20 °C and the whole ionic concentration is 0.1 mol/L.

II. EXPERIMENTS

A. Electroless deposition of the CNTs

The multi-walled carbon nanotubes (MWCNTs) with purity about 95% were produced via catalytic decomposition of hydrocarbon which was provided by Shenzhen Nanotech Port Company. Prior to electroless plating, the MWCNTs must be pretreated by two steps: purification and ball milling. In the purification process, the MWCNTs were added to a mixed solution of sulphuric acid and potassium dichromate (0.38 mol/L K_2CrO_7+4.5 mol/L H_2SO_4) and immerged in a 60 °C water bath for 6 h so as to oxidize the dirt nanotubes . Then, the purified MWCNTs were washed and dried. The ball milling of the purified MWCNTs was carried out using a GN-2 type ball mill at 200 r/min for 15 h for better dispersion. Hardened steel balls of 12 mm diameter were employed as the ball milling medium.

The whole process of electroless deposition was done in steps as shown in Fig.1. The optimum electroless plating conditions are shown in Table I, which were determined by orthogonal experiments. Nine of Co^{2+} to Ni^{2+} ratios were chosen for the investigation, *i.e.* 1/5, 1/4, 1/3, 1/2, 1/1, 2/1, 3/1, 4/1, and 5/1 respectively. The deposition rate was obtained by measuring the coating weight per square centimeter. After plating, the samples were heat-treated under hydrogen atmosphere at 450 °C for 1 h.

B. Characterization of the products

The coated MWCNTs were carefully collected, and then were characterized and analyzed by X-ray diffraction (XRD, D/MAX-B with Cu Kα, λ=0.15418 nm), field-emission scanning electron microscopy (FESEM, JEOL JSM-6700F), transmission electron microscopy (TEM, Hitachi Model H-800), energy dispersive X-ray spectroscopy (EDS) (EDAX, DX-4), and a vibrating sample magnetometer (MPMS-XL 5 SQUID Magnetometer).

III. RESULTS AND DISCUSSION

A. Effects of deposition parameters on the deposition rate

1. Effect of the concentration ratio of Co^{2+}/Ni^{2+}

Co and Ni can be co-electrodeposited to form alloy coatings because their standard electrode potentials are very close. In fact, cobalt is more difficult to reduce owing to its lower potential compared with nickel. Therefore, the deposition rate is obviously influenced by the concentration ratio of cobalt ion to nickel ion (Co^{2+}/Ni^{2+}) in the electroless deposition solution. Figure 2 gives the relationship between the deposition rate and Co^{2+}/Ni^{2+} value, when the solution pH value is 8.5, bath temperature is 20 °C and the whole ionic concentration is 0.1 mol/L. It can be seen that the deposition rate of Co-Ni-P coatings increases with the increase of Co^{2+} relative content when the Co^{2+}/Ni^{2+} value is less than 1; and the deposition rate reaches the maximum

DOI:10.1088/1674-0068/22/04/411-416

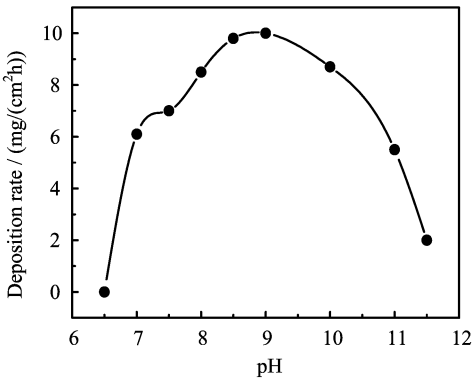

FIG. 3 Variation of the deposition rate at various solution pH values with Co^{2+}/Ni^{2+} ratio 1 and bath temperature 20 °C.

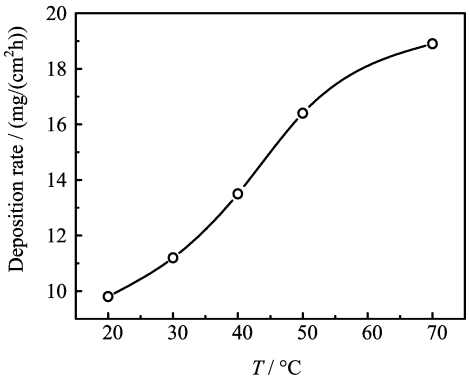

FIG. 4 Variation of the deposition rate at different bath temperatures with Co^{2+}/Ni^{2+} ratio 1 and solution pH 8.5.

value when the Co^{2+}/Ni^{2+} ratio is 1/1; while the deposition rate decreases with the increase of Co^{2+} relative content when the Co^{2+}/Ni^{2+} ratio is greater than 1/1.

2. Effect of the solution pH value

The effect of the solution pH value on the deposition rate is shown in Fig.3, when the Co^{2+}/Ni^{2+} ratio is 1/1 and bath temperature is 20 °C . It can be seen that the deposition rate is very low in the acid solution, and the deposition hardly occurs when the pH value is less than 6.5. As the solution pH value becomes greater than 6.5, the reduction ability of NaH_2PO_2 gradually becomes stronger, which results in the increase of the deposition rate of Ni-Co-P coatings. The deposition rate shows a peak around pH 9.0. When the solution pH value is greater than 9.0, the deposition rate begins to decrease. If the pH value is higher than 11.5, it is easy to separate out white precipitates of $Co(OH)_2$ leading to the failure of the electroless deposition solution. Therefore, the appropriate pH value for the deposition of Ni-Co-P coatings should be controlled in the range of 8.5–8.8.

3. Effect of the bath temperature

The experimental results of the deposition rates varying with the bath temperatures (pH=8.5, Co^{2+}/Ni^{2+}=1) are shown in Fig.4. The data indicate that the deposition rate increases monotonically with the increase of the bath temperature. At higher temperatures, the higher deposition rate will readily lead to the newly reduced metallic particles accumulating on the formerly deposited particles, thus forming coarse particles attached to the MWCNTs, which results in the formation of a nonuniform Ni-Co-P coating on the CNTs. For this reason, the low deposition rate is desired to form ideal uniform Ni-Co-P coatings on the MWCNTs, so the favorable bath temperature range of 15–25 °C is chosen for the eletroless plating of

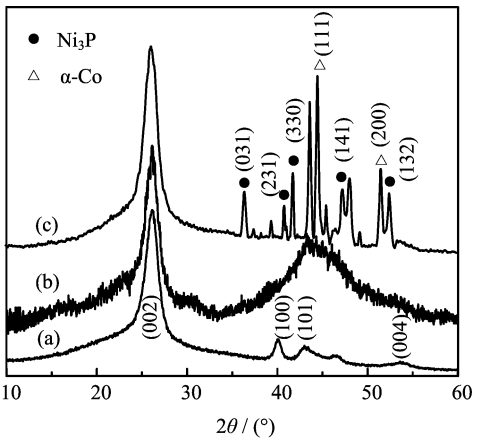

FIG. 5 XRD patterns of MWCNTs: (a) before electroless plating (purified state), (b) after electroless plating with Ni-Co-P alloy, and (c) heat-treated products (450 °C, 1 h).

the Ni-Co-P alloy coatings on the MWCNTs.

B. Structure and morphology of as-coated MWCNTs

The structures of the uncoated and coated MWCNTs were analyzed by XRD. Figure 5 shows the XRD spectra of MWCNTs before and after electroless plating with Ni-Co-P alloy coatings. The XRD spectrum of the purified MWCNTs by sulphuric acid and potassium dichromate is shown in Fig.5(a). It was difficult to find impurities in the products, but the graphitization degree of the MWCNTs is very high. Four diffraction peaks are found corresponding to (002), (100), (101) and (004) planes of crystalline state graphite (according to JCPDS: 41-1487). An amorphous peak at 2θ=45° is observed in the spectrum of the plated MWCNTs, indicating that Ni-Co-P alloy coatings under the plating state are amorphous (Fig.5(b)). It was proved that the amorphous nature of the deposits of Ni-P still remains when the temperature of heat treatment is below 300 °C according to Ref.[34]. When the temperature of

DOI:10.1088/1674-0068/22/04/411-416

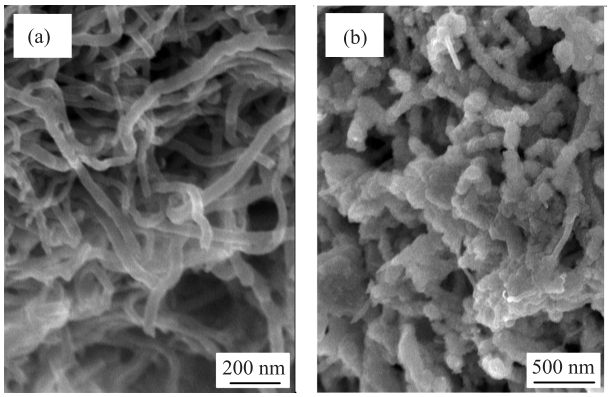

FIG. 6 Typical SEM images of MWCNTs: (a) before electroless plating (purified state), (b) after 30 min electroless plating with Ni-Co-P alloy.

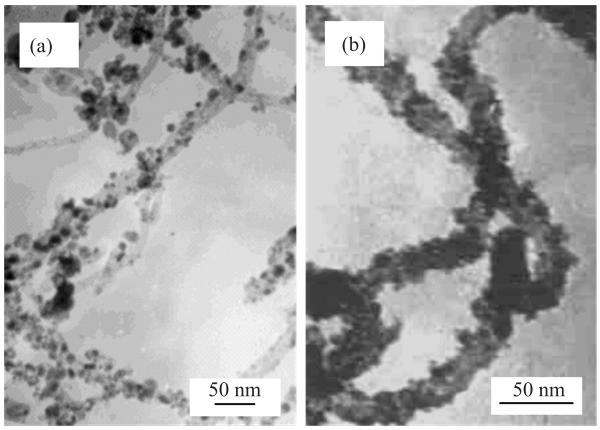

FIG. 7 TEM images of MWCNTs plated with Ni-Co-P alloy at different deposition times: (a) 15 min, (b) 30 min.

heat treatment exceeds 400 °C, the Ni phase and the Ni_3P phase increase strongly. In order to obtain crystal structure of the Ni-Co-P alloy coatings, the as-coated products were heat-treated at 450 °C for 1 h. The XRD spectrum obtained from the heat-treated sample shows sharp, well-defined peaks corresponding to a fully crystallized structure (Fig.5(c)). The five peaks at 2θ=36.38°, 41.88°, 42.78°, 46.68°, and 52.88° represent the well-defined peaks corresponding to diffraction from (031), (231), (330), (141), and (132) planes, respectively, of the Ni_3P (according to JCPDS: 34-501). The two peaks at 2θ=44.48° and 51.78° represent peaks corresponding to diffraction from (111) and (200) planes, respectively, of the α-Co (according to JCPDS: 01-1254). The result reveals the heat-treated Ni-Co-P coatings on MWCNTs have crystalline structure.

The morphology of the plated MWCNTs was further characterized by the SEM and the TEM. The typical SEM images of MWCNTs before and after electroless plating are shown in Fig.6 (a) and (b) respectively. It can be seen that the purified MWCNTs are very clean and smooth (Fig.6(a)). After electroless plating with Ni-Co-P alloy, the MWCNTs are well wrapped with a thin rough layer (Fig.6 (b)). The TEM observations revealed the plating process at different deposition times. It is found in Fig.7(a) (at 15 min) that the alloy particles begin to selectively precipitate in the activated points on the MWCNTs surface and the MWCNTs are partially coated by the alloy particles. After 30 min plating, the uniform, integrated and high quality Ni-Co-P alloy films are obtained and almost all the surface of MWCNTs is successfully coated by alloy coatings, as shown in Fig.7(b) (at 30 min).

C. Magnetic properties of as-coated MWCNTs

Magnetic properties of the Ni-Co-P alloy coated MWCNTs were characterized by a vibrating sample magnetometer. The magnetic properties such as coercivity (H_c), magnetic conductivity (μ_m), magnetic saturation (M_s), and remnant magnetization (M_r) were obtained at different Co^{2+} to Ni^{2+} values from 1/5 to 5/1. The measured results are shown in Fig.8.

It has been proved that the 3d electron wave functions of neighboring atoms in 3d transition metals show a strong overlap [35], which leads to 3d electron bands rather than to 3d levels. The carriers of magnetism in iron, cobalt and nickel are the holes in these 3d bands. In Ni-Co alloys, the addition of Co leads to the redundant d electrons, which will enter the positive spin bands, and give rise to the increase of the positive spinning electrons, to increase the magnetic moment.

It can be seen in Fig.8(a) that the change of the M_s is small when the Co^{2+}/Ni^{2+} value is smaller than 1. As the Co^{2+}/Ni^{2+} value exceeds 1, the positive spinning electrons increase obviously with the increase of Co^{2+}/Ni^{2+} value, which results in the rapid increase of M_s of the products. As the number of the positive spinning electrons reaches the maximum value, the products have a maximum M_s (at Co^{2+}/Ni^{2+}=2/1). After that, M_s decreases as the Co^{2+}/Ni^{2+} value gets bigger. Meanwhile, as compared with M_s, the increase of the M_r with the variation of Co^{2+}/Ni^{2+} value is slight. A comparison of the magnetic characteristics of electroless Ni-Co-P deposits in Sankara Narayanan's study also showed that the saturation magnetization and remanence are found to increase with cobalt content of the deposit [34]. An earlier report found a linear increase in magnetic moment with increase in cobalt content for electrodeposited Ni-Co-P amorphous ribbons [36]. An increase in saturation magnetization of electroless Ni-Co-P deposits with increase in cobalt content of the deposit was also reported by Matsubara and Yamada [37].

As for H_c, in the obtained curve there exist two peaks corresponding to Co^{2+}/Ni^{2+} value being 1/3 and 4/1. H_c depends mainly on the resistances to the ir-

DOI:10.1088/1674-0068/22/04/411-416

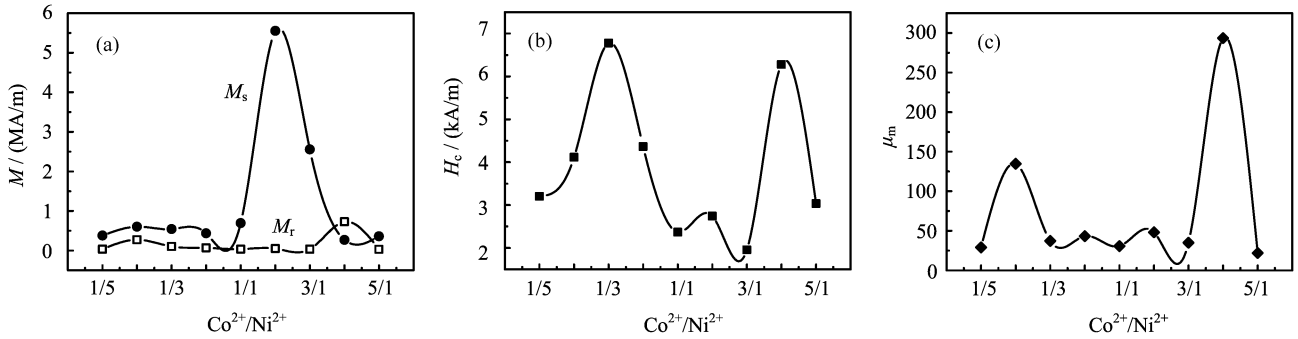

FIG. 8 Composition dependences of the magnetic properties of the Ni-Co-P coated MWCNTs: (a) magnetic saturation (M_s) and remanent magnetization (M_r) of the products at different Co^{2+}/Ni^{2+} values, (b) coercivity (H_c), and (c) magnetic conductivity (μ_m).

reversible displacement of the magnetic domain wall and the rotation of the magnetic domain. The bigger the resistances, the higher the H_c is. Simpson and Brambley appear to have been the first to point out that the amorphous alloys, expected to have no magnetocrystalline anisotropy, should have very low coercivities [38]. However the early amorphous alloys of CoP, prepared by deposition methods, had coercivities as high as 800–1600 A/m. These high coercivities are now understood to arise from compositional inhomogeneities demonstrated by Chi and Cargill [39] from small angle X-ray scattering analysis and from strain-magnetostriction anisotropy. According to this explanation, the two H_c peaks in Fig.8(b) are attributed to compositional inhomogeneities in the alloys.

It is well known that the μ_m is dominated mainly by the difficulty degree in reversible magnetization. If the reversible displacement of the magnetic domain wall and the rotation of magnetic domain occur easily, then the μ_m will be high, and vice versa [40]. When the Ni and Co are co-deposited, a solid solution reaction will take place between Ni and Co. The change of the content of the components in the alloy will lead to lattice distortions and the increase of defects (grain boundary, stacking-fault, etc.), affecting the fluctuation in anisotropy. When the contents of Ni and Co are close, the produced lattice distortion is the greatest, causing the severe pinning of the magnetic domain walls, *i.e.* it is difficult for magnetic domain walls to move, and μ_m will become smaller, as seen in Fig.8(c); μ_m is the lowest when Co^{2+}/Ni^{2+} is 1. There are two μ_m peaks corresponding to greater Ni or Co content owing to the easiest magnetization conditions. The effect of Co on the μ_m is stronger than that of Ni, because the higher peak is caused by the greater Co content.

IV. CONCLUSION

In summary, MWCNTs were successfully coated with a layer of Ni-Co-P alloy with different composition of Ni/Co through electroless plating. The effects of the concentration ratio of Co^{2+} to Ni^{2+}, bath temperature and pH on deposition rate are discussed. The results show that the deposition rate reached the maximum when the concentration ratio of Co^{2+} to Ni^{2+} is 1. Also, the maximum deposition rate appears at pH being 9, and the deposition rate increases with the increase of bath temperature. The prepared MWCNTs covered with Ni-Co-P using the optimized deposition conditions were characterized and analyzed. The SEM and TEM observations revealed that all the MWCNTs were uniformly covered with a layer of Ni-Co-P alloy. The XRD analysis showed that the as-coated products were amorphous, and changed into crystal structure after heat treatment at 450 °C for 1 h. The measurements of the magnetic properties of the obtained CNTs covered with Ni-Co-P thin layer indicates that the magnetic properties greatly depend on the concentration ratio of Co^{2+} to Ni^{2+}, *i.e.* the magnetic saturation (M_s) reaches the maximum value when Co^{2+} to Ni^{2+} is 1. In addition, there are two peaks in the coercivity (H_c) curve at Co^{2+} to Ni^{2+} ratios 1/3 and 4/1 respectively, while the two peaks in the magnetic conductivity (μ_m) curve are located at Co^{2+} to Ni^{2+} ratios 1/4 and 4/1.

V. ACKNOWLEDGMENTS

This work was supported by the National Major Project of Fundamental Research: Nanomaterials and Nanostructures (No.2005CB623603) and the National Natural Science Foundation of China (No.10674138).

[1] S. Iijima, Nature **354**, 56 (1991).
[2] R. Saito, G. Dresselhaus, and M. Dresselhaus, *Physical Properties of Carbon Nanotubes*, London: Imperial College Press, (1998).
[3] M. A. Reed, *Molecular Electronics*, London: Academic Press, (2000).

DOI:10.1088/1674-0068/22/04/411-416

[4] J. Kong, N. R. Franklin, C. Zhou, G. M. Chapline, S. Peng, D. Kyeongjae, and H. J. Dai, Science **287**, 622 (2000).
[5] S. S. Wong, A. T. Woolley, E. Joselevich, C. L. Cheung, and C. M. Lieber, J. Am. Chem. Soc. **120**, 8557 (1998).
[6] C. Niu, E. K. Sichel, R. Hoch, D. Moy, and H. Tennent, Appl. Phys. Lett. **70**, 1480 (1997).
[7] E. Frackowiak, S. Gautier, H. Gaucher, S. Bonnamy, and F. Beguin, Carbon **37**, 61 (1999).
[8] P. Ayala, W. Plank, A. Gruneis, E. I. Kauppinen, M. H. Rummeli, H. Kuzmany, and T. Pichler, J. Mater. Chem. **18**, 5676 (2008).
[9] K. P. Gong, F. Du, Z. H. Xia, M. Durstock, and L. M. Dai, Science **323**, 760 (2009)
[10] R. T. Lv, F. Y. Kang, J. L. Gu, X. C. Gui, J. Q. Wei, K. L. Wang, and D. H. Wu, Appl. Phys. Lett. **93**, 223105 (2008).
[11] O. V. Kharissova, M. G. Castanon, J. L. Hernandez Pinero, U. O. Mendez, and B. I. Kharisov, Mech. Adv. Mater. Struc. **16**, 63 (2009).
[12] L. Zhang and H. Zhu, Mater. Lett. **63**, 272 (2009).
[13] J. Lee, W. Lee, K. Sim, S. H. Han, and W. Yi, J. Vac. Sci. Technol. B **26**, 1892 (2008).
[14] S. Mao, G. H. Lu, and J. H. Chen, Nanotechnology **19**, 455610 (2008).
[15] H. F. Cui, J. S. Ye, W. D. Zhang, and F. S. Sheu, Biosens Bioelectron **24**, 1723 (2009).
[16] D. Tasis, N. Tagmatarchis, A. Bianco, and M. Prato, Chem. Rev. **106**, 1105 (2006).
[17] X. Hu and S. Dong, J. Mater. Chem. **18**, 1279 (2008).
[18] B. Xue, P. Chen, Q. Hong, J. Lin, and K. L. Tan, J. Mater. Chem. **11**, 2378 (2001).
[19] H. Q. Wu, D. M. Xu, Q. Wang, Q. Y. Wang, G. Q. Su, and X. W. Wei, J. Alloy. Compd. **463**, 78 (2008).
[20] X. Hu, T. Wang, X. Qu, and S. Dong, J. Phys. Chem. B **110**, 853 (2006).
[21] Y. Zhang, N. W. Franklin, R. J. Chen, and H. Dai, Chem. Phys. Lett. **331**, 35 (2000).
[22] Q. Q. Li, S. S. Fan, W. Q. Han, C. H. Sun, and W. J. Liang, Jpn. J. Appl. Phys. **36**, L501 (1997).
[23] L. M. Ang, T. S. A. Hor, G. Q. Xu, C. H. Tung, S. P. Zhao, and J. L. S. Wang, Carbon **38**, 363 (2000).
[24] C. Sangregorio, C. D. Fernandez, G. Battaglin, G. De, D. Gatteschi, G. Mattei, and P. Mazzoldi, J. Magn. Magn. Mater. **272**, E1251 (2004).
[25] S. K. Lim, K. S. Ban, Y. H. Kim, C. K. Kim, C. S. Yoon, and S. Jin, Appl. Phys. Lett. **88**, 163102 (2006).
[26] F. Branda, G. Luciani, M. Leoni, A. Costantini, B. Silvestri, and P. Scardi, Appl. Phys. A **90**, 695 (2008).
[27] K. S. Lew, M. Rajab, S. Thanikaikarasan, T. Kim, Y. D. Kim, and T. Mahalingam, Mater. Chem. Phys. **112**, 249 (2008).
[28] X. Y. Yuan, G. S. Wu, T. Xie, Y. Lin, G. W. Meng, and L. D. Zhang, Solid State Commun. **130**, 429 (2004).
[29] S. L. Cheng and C. N. Huang, Syn. React. Inorg. Met., **38**, 475 (2008).
[30] S. Guan and B. J. Nelson, J. Electrochem. Soc. **152**, C190 (2005).
[31] K. Itakura, T. Homma, and T. Osaka, Electrochim. Acta **44**, 3707 (1999).
[32] S. Djokic, J. Electrochem. Soc. **146**, 1824 (1999).
[33] Y. Li, R. Wang, F. Qi, and C. Wang, Appl. Surf. Sci. **254**, 4708 (2008).
[34] T. S. N. Sankara Narayanan, S. Selvakumar, and A. Stephen, Surf. Coat. Technol. **172**, 298 (2003).
[35] E. P. Wohlfarth, *Ferromagnetic Materials-A Handbook on the Properties of Magnetically Ordered Substances*, Amsterdam: North-Holland Publishing Company, (1980).
[36] G. Rivero, M. Multigner, J. M. Garcia, P. Crespo, and A. Hernando, J. Magn. Magn. Mater. **177-181**, 119 (1998).
[37] H. Matsubara and A. Yamada, J. Electrochem. Soc. **141**, 2386 (1994).
[38] A. W. Simpson and D. R. Brambley, Phys. Stat. Sol. (b) 4**3**, 291 (1971).
[39] G. C. Chi and G. S. Cargill III, Mater. Sci. Eng. **23**, 155 (1976).
[40] G. Herzer, *Handbook of Magnetic Materials*, Amsterdam: Elsevier, (1997).

DOI:10.1088/1674-0068/22/04/411-416